ISBN: 978-3-95450-214-1 ISSN: 2673-5490 doi:10.18429/JACoW-IPAC2021-THPAB307

BEHAVIOUR OF IRONLESS INDUCTIVE POSITION SENSORS IN CLOSE PROXIMITY TO EACH OTHER*

N. Sammut†[1], A. Grima[1], the University of Malta, Msida, Malta
M. Di Castro, A. Masi, the European Organisation for Nuclear Research, Geneva
[1]also at the European Organisation for Nuclear Research, Geneva

Abstract

Safety critical systems like the collimators of the Large Hadron Collider require transducers which are immune to interference from their surroundings. The ironless inductive position sensor is used to measure the position of collimator jaws with respect to the beam and is designed to be immune to external DC or slowly changing magnetic fields. In this paper we investigate whether frequency separation is required when multiple ironless inductive position sensors are used and whether two or more sensors at the same frequency results in cross-talk. Numerical simulations and experiments are conducted to study the magnetic field behaviour of the sensors, their interference with each other and the impact of this interference on the position reading. Finally, this paper defines guidelines on safe operation of the ironless inductive position sensor in the aforementioned conditions.

INTRODUCTION

In the Large Hadron Collider (LHC) at the European Organisation for Nuclear Research (CERN), the collimators are part of the critical machine protection system making it paramount that the measurements from the collimation sensors are not affected by magnetic fields [1] originating from the surrounding environment [2, 3]. Furthermore, since a collimator sets the diagonal dimension of the beam, it is very important that the jaw position is very accurate. The nominal beam size at the collimator is 200 μm and the maximum target position uncertainty of the jaws is set to be 20 μm i.e. one tenth of the nominal beam size. These conditions provide a challenge to the sensor and electronics design. Linear position sensors are used to measure the jaw position with respect to the beam at all times [4, 5]. The two linear position sensors used for this job are the Ironless Inductive Position Sensors (I2PS) and the Linear Variable Differential Transformers (LVDT) [6]. It has been shown that the LVDTs [7] suffer from significant electromagnetic interference when placed in environments characterised with dc or slowly varying magnetic fields [1, 3, 8] mainly due to the magnetically permeable core. Since the design of the I2PS is based on air-cored coils and a non-contact moving coil, the I2PS is basically immune to slowly varying magnetic fields (< 1 Hz). This makes the I2PS [9] a valid substitute of the LVDT which is currently the typical position sensor used in the LHC collimators when high-precision position measurements are required.

* Work supported by CERN – The European Organisation for Nuclear Research, and the University of Malta
† nicholas.sammut@um.edu.mt

A collimator requires a total of seven linear position sensors. Even though the I2PS is found to be immune to dc or slowly varying magnetic fields, all the seven sensors installed in the collimator are operated at a different frequency (starting from 750 Hz to 2250 Hz at 250 Hz intervals) to minimise the risk of electromagnetic cross-talk when they are close to each other. This paper investigates the necessity of frequency separation from a transducer point of view [10] by investigating whether operating two or more sensors at the same frequency (e.g. 1 kHz) results in cross-talk. This work also aims at defining a safe distance at which several I2PS can be operated at the same frequency without causing interference to each other.

SENSOR'S FINITE ELEMENT MODEL

The design and working principle of the I2PS is well documented in [11]. The supply coils are usually operated with an ac current supply with a maximum current of 50 mA peak at 1 kHz. It is understandable that the lower the magnetic field propagated by the I2PS to the surroundings, the lower the possible effect on the coils. A finite element simulation is used to understand how far the magnetic field propagates around the sensor and how it behaves at the edges of and in between the two sensors. This allows an understanding of the distance required to place a second I2PS. The Finite Element Model (FEM) [12, 13] of the I2PS is built using the simulator FLUX® developed by Altair in both 2D and 3D. This is done since in FLUX® a 2D simulation can either be a 2D diagram which is either prolonged or revolved. For the I2PS which is an axisymmetric sensor, a 2D simulation can be used as long as this condition is maintained. Hence, in a 2D axisymmetric simulation, one-half of the device is defined in the study domain, and the software revolves it around the symmetry axis. This results in a less computationally intensive simulation with respect to the 3D one, whilst as noted in the past [13], still obtaining a 98% match with the 3D simulation. For these simulations, as long as the change in the I2PS' position with respect to each other is only in the y-axis, a 2D simulation can be performed. The addition of a second sensor in the x-direction transforms the domain in a non-axisymmetric one and hence requires a transient-magnetic 3D simulation. Henceforth, two sensors are used for the tests referred to as $I2PS_{S1}$ and $I2PS_{S2}$.

The 3D simulated sensors are built with a fusion of meshed and non-meshed coils. A non-meshed coil superimposes on the available mesh and consequently it is independent from it. The main benefit obtained from this

ISBN: 978-3-95450-214-1 ISSN: 2673-5490 doi:10.18429/JACoW-IPAC2021-THPAB307

type of coil is a significant reduction of the number of nodes. Conversely, it requires that the available mesh is fine such that the accuracy remains high. This combination ensures a high percentage of excellent quality elements in the mesh whilst the number of nodes/elements is decreased. The lower the number of nodes, the lower the time and the computational resources required for the simulation to finish. The dimensions of the sensor and its coils are documented in [11]. The thinnest coil of the I2PS is the sense coil ≈ 0.3 mm, hence, it is set to a meshed coil whilst the moving and supply coils are set to non-meshed coils. Consequently, the sense coil is set to a mesh with 0.15 mm tetrahedrons, generating a fine mesh that the non-meshed coils can superimpose on. In fact, this places the non-meshed coils inside the area meshed with elements ranging from 0.15 mm to 1.5 mm. Since, the supply coil is thicker and only 0.05 mm away from the sense coil, the mesh relaxation does not affect the simulation accuracy. Furthermore, the moving coil has a bigger diameter and hence a bigger mesh (1.5 mm) can be used. The shield is set to a meshed solid and meshed with 5 mm elements.

Flux® suggests that at least two elements are placed in any direction. When Flux® is used for a transient electromagnetic simulation, it interfaces shapes in the designer to electronic components in a circuit designer. In this way the coils' electrical characteristics can be defined and a circuit is created which interacts with the Finite Element Model (FEM). The separate components are connected together or to other components such as supply and acquisition circuits, creating an electrical circuit within the FEM. Two current supplies are set to generate opposite 50 mA - peaks with a frequency of 1 kHz and these are connected to the supply coils. Coil conductors are used to link the coils in the geometry with the one in the electrical network. In the electrical model the supply coil's resistance is set to 55 Ω. The sense coils' resistance is set to 2.5 kΩ. Since, a very high impedance readout system is used to read the signal from the sense coils, a resistor of 1 MΩ is placed in parallel. The moving coil's resistance is set to 17.9 mΩ and a resistor of 1 mΩ is set in parallel to it to simulate the short.

Numerical Simulation Results

The results presented show the magnetic field when $I2PS_{S1}$ and $I2PS_{S2}$ are parallel to each other and $\Delta x = 1$ cm. These results also present the case where the moving coils are in the same position inside the sensor and the supply phase is the same. The selected state is presented since it is observed that it is the condition that creates the highest field between the two. It is observed that the magnetic field oscillates, as expected, with the frequency of the sensors.

The graph presented in Fig. 1 shows the magnetic field along the sensors at different points. In Flux®, path lines can be set to take a cross section of the amplitude of a parameter; in this case of the magnetic field. To understand the curves presented better, the position of the coils inside the sensor are marked in lines at the top of the graph. Five paths are considered; a path between the two sensors and paths at 5 mm, 10 mm and 20 mm away from the sensor.

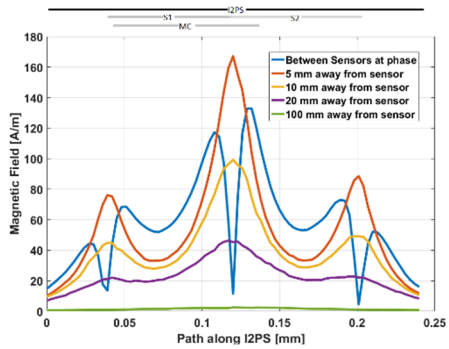

Figure 1: Magnetic field at increasing distances from the sensor at the peak of the supply current. Note that the lines above the graph is an accurate definition of the location of any one of the sensors (since they are parallel) and its major components which matches to the position presented in the x-axis.

Starting from the curve 5 mm away from $I2PS_{S2}$ the magnetic field has three peaks along the $I2PS_{S2}$ at the ends of the sense/supply coils and at the small gap between the coils at the centre of the sensor. This 1 mm gap between the two sense and supply coils comes from the manufacturing process and cannot be removed. Moving away from the centre, two more peaks can be noted at the end of the sense/supply coils. Note that these curves are taken outside any of the sensors and hence only the magnetic field of one sensor is observed.

It is also observed that the peak that coincides with the start of the moving coil (MC) is smaller than the one on the opposite end by 12 A/m. This is because the moving coil generates a field opposite to that generated by supply coils hence attenuating the overall magnetic field. As the path is moved, further away from the sensor, the magnetic field decreases. The curve taken 10 mm outside the sensor is very similar to that of 5 mm away but with a smaller amplitude. In the case of the curve between $I2PS_{S1}$ and $I2PS_{S2}$, this path is set at 5 mm away from each sensor. In this case, multiple peaks form close to the beginning and ends of the coils. A sharp drop in the magnetic field is noted at the air-gap between S1 and S2 whilst the biggest peak is observed at one end of the moving coil. To note that the shape of the curve is very similar to that of 5 mm and 10 mm away from the sensor. It can be deduced that the magnetic field's drop results from the interaction of the magnetic fields of the two sensors. A similar but much smaller effect can be noted when the amplitude of the supply of the sensor is at the zero point. In this case, the simulations show a very weak interaction outside the sensor. We can also consider the case where the sensors are in series with each other rather than in parallel. This means that there is no Δx, but they are centred and there is a $\Delta y = 5$ mm. In this case, the behaviour is very similar to that experienced when the sensors are parallel to each other. The deduction that the moving coil causes inequality in the side peaks as presented in Fig. 1 is proven in Fig. 2. The two side peaks have the same magnitude since the moving coils are set in the middle of the sensor. Moreover,

ISBN: 978-3-95450-214-1 ISSN: 2673-5490 doi:10.18429/JACoW-IPAC2021-THPAB307

between the sensors, the amplitude of the magnetic field is reduced to approximately 10 A/m. In the centre, the magnitude falls to almost zero hence the magnetic field from both sensors cancels out.

The simulation results show that an oscillating magnetic field is present between and around the sensors. The simulation also shows that the magnetic field is not small but it decreases rapidly with distance from the I2PS. In fact, the paths show that there should be a negligible magnetic field 100 mm away from the sensor.

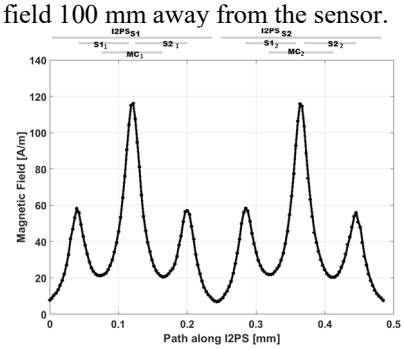

Figure 2: Magnetic field along two sensors which are in series to each other. Note that above the figure an accurate definition of the location of the sensors and their major components is presented which matches to the position presented in the x-axis.

TEST-BENCH RESULTS

A simple test bench is set-up to test the impact of the magnetic field on the position read by the sensors. $I2PS_{S1}$ is first left at the zero point of the ruler. In these measurements, the moving coil is centred but left free to move. The other sensor, $I2PS_{S2}$ is moved to the position required away from $I2PS_{S1}$. When the $I2PS_{S2}$ is in position, the acquisition is started to obtain a baseline without interference and then the supply of $I2PS_{S2}$ is turned on.

Figure 3 presents the amplitude of the sense coils' voltage when the $\Delta x = 10$ mm. The power supply of the second I2PS is turned on after two seconds. Note that in this time window there is no change in voltage. When the $I2PS_{S2}$ is turned on there is a sudden voltage drop of 0.1 V and then it starts changing sinusoidally with a ΔV of max 0.24 V at a very slow rate of 0.03 Hz. This results in a ± 250 µm of position change as indicated in Fig. 4. Note that the position change remains at the same frequency but decreases in amplitude the further away they are from each other. While the position change of the sensor is appreciably smaller when $I2PS_{S1}$ and $I2PS_{S2}$ are $\Delta x = 100$ mm apart, the I2PS still suffers a position change of 50 µm. The amplitude of the interference continues to decrease until the position drift is not obvious any more. On the scale of Fig. 4 this happens when the sensors are 300 mm apart. Further examination of the position change when the sensor is 350 mm away from each other in the x-axis shows that at this distance there is still interference, yet it has decreased to approximately 1 µm and hence can be deemed negligible.

The process is repeated when the I2PS is moved in both the x-plane and the y-plane. In this case, since the sensor is moved in the y-axis, there is no change in the level of interference between the two.

These results lead to the final test which is conducted on a test collimator. Multiple collimators can be found at CERN outside the LHC tunnel used as a test setup. These are configured in exactly the same way as the ones in the LHC and are used for compliance and new systems tests. For this test, three out of six jaw sensors are set to operate at 1 kHz. These three sensors are the Right Upstream, the Right Downstream, and the Left Downstream. The other three i.e. the two Gap sensors and the Left Upstream are set at 1.25 kHz; 1.5 kHz and 1.75 kHz respectively. This selection provides different distances between the sensors and also different objects separating them. It is noted from this test that no interference is noted on these sensors implying that the six sensors associated with the jaws can be operated at only two frequencies.

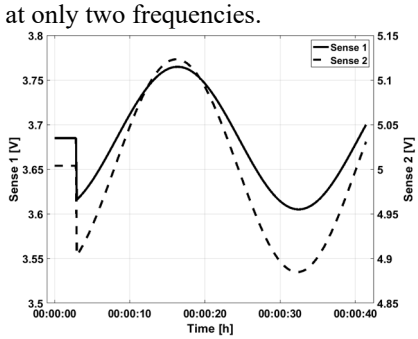

Figure 3: Comparison of the Sense coils' voltages with interference when $\Delta x = 10$ mm as obtained from the test-bench.

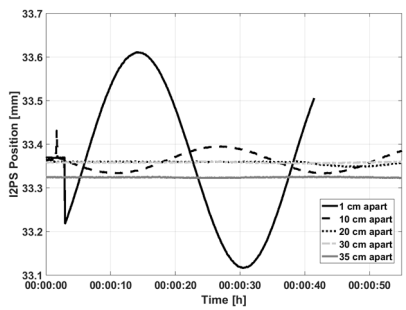

Figure 4: Comparison of the position reading with interference at different Δx distances between the two I2PS as obtained from the test-bench.

CONCLUSION

The effect of two sensors operated in close proximity at the same frequency are presented in this paper. The results show that whilst the I2PS is found to be immune to DC or slowly varying magnetic fields, it is in fact susceptible to cross-talk from other I2PS sensors operating at the same frequency (for example both sensors operate at 1 kHz). However, the magnetic field produced by an I2PS is low enough to decrease sufficiently by 100 mm. At this distance, the position change is less than 50 µm. This study shows that the safe distance for these sensors to be operated at the same frequency (in this case of 1 kHz) is 350 mm. Finally, this work presents the implementation of the frequency setting on a test collimator which shows that there is no interference between the three sensors.

ISBN: 978-3-95450-214-1 ISSN: 2673-5490 doi:10.18429/JACoW-IPAC2021-THPAB307

REFERENCES

[1] A. Danisi, "Simulation of dc interfering magnetic field effects on the LHC collimators' LVDT positioning sensors" M. Sc. Thesis, Electronic Engineering Department, University of Naples "Federico II", Naples, Italy, 2009.

[2] A. Masi *et al.,* "Study of magnetic interference on an LVDT: FEM Modeling and Experimental Measurements", *J. Sens.*, vol. 2011, pp. 529454-1—529454-9, May 2011. doi:10.1155/2011/529454

[3] M. Martino *et al.*, "Design of a linear variable differential transformer with high rejection to external interfering magnetic field", *IEEE Trans. Magn.,* vol. 46 (2), pp. 674-677, Feb. 2010. doi:10.1109/TMAG.2009.2033341

[4] T. Weiler *et al.*, "LHC Collimation System Hardware Commissioning", *In Proc. PAC'07*, Albuquerque, USA, Jun. 2007, paper TUPAN108, pp 1625-1627. doi:10.1109/PAC.2007.4440844

[5] R. Assmann *et al.*, "LHC collimation: design and results from prototyping and beam tests", *in Proc. PAC'05*, Knoxville Tennessee, May 2005, pp 1078-1080. doi:10.1109/PAC.2005.1590664

[6] A. Danisi *et al.*, "Design optimization of an ironless inductive position sensor for the LHC collimators", *JINST,* vol. 8, p. P09005, Sept. 2013. doi:10.1088/1748-0221/8/09/P09005

[7] D. S. Nyce, *Linear Position Sensors: Theory and Application.* Hoboken, New Jersey, USA: John Wiley & Sons, 2004.

[8] M. Martino *et al.*, "An analytical model of the effect of external dc magnetic fields on the ac voltages of an LVDT." *In Proc. IMTC2010*, Austin, Texas, USA, May 2010, pp. 213-218, 2010. doi:10.1109/IMTC.2010.5488116

[9] A. Masi *et al.*, "Ironless position sensor with intrinsic immunity to external magnetic fields", in *Proc. IEEE Sensors*, Limerick, Ireland, Oct. 2011, pp. 2018-2021. doi:10.1109/ICSENS.2011.6127118

[10] A. Danisi, "Ironless Inductive Position Sensor for Harsh Magnetic Environments", Ph.D. thesis, Ecole Polytechnique Federale de Lausanne, Lausanne, Switzerland, 2013.

[11] A. Grima *et al.*, "Influence of external conductive objects on the performance of an ironless inductive position sensor", *IEEE Sensors Journal*, vol. 17, no. 14, pp. 4500–4507, Jul. 2017. doi:10.1109/JSEN.2017.2708320

[12] J. Sylculslci *et al.*, "Application of Finite element modelling in LVDT design", *COMPEL*, vol. 11, no. 1, pp. 73–76, Jan. 1992. doi:10.1108/eb051755

[13] M. Křížek and P. Neittaanmäki, *Mathematical and Numerical Modelling in Electrical Engineering Theory and Applications*. Dordrecht, Netherlands: Springer Netherlands, 1996.